



## Adsorption characteristics of Ni<sup>2+</sup> ion onto the diethylenetriaminepentaacetic acid-melamine / polyvinylidene fluoride blended resin

Xiaodan Zhao, Laizhou Song, Jun He, Tingying Wu, Ying Qin

Department of Environmental and Chemical Engineering, Yanshan University, Qinhuangdao 066004, China.

### Abstract

The polyvinylidene fluoride blended resin (DTPA-MA/PVDF) adsorbent prepared by anchoring the chelating agent diethylenetriaminepentaacetic acid (DTPA) to the resin via the amide covalent bond reaction between DTPA and melamine(MA), was used to remove nickel from aqueous solutions. The blended resin was prepared using the combination of solution blending technique and phase inversion process. The blended resin was characterized by Fourier transform infrared spectroscopy (FTIR), <sup>13</sup>C nuclear magnetic resonance spectroscopy (<sup>13</sup>C NMR), environmental scanning electron microscopy (ESEM) and N<sub>2</sub> adsorption/desorption experiments. The sorption data was fit to linearized adsorption isotherms of the Langmuir, Freundlich, and D-R isotherms models. The batch sorption kinetics was evaluated using pseudo-first-order, pseudo-second-order, and intraparticle diffusion kinetic reaction models.  $\Delta H^\circ$  is less than 0,  $\Delta G^\circ$  is lower than 0, and  $\Delta S^\circ$  is greater than 0, which shows that the adsorption of Ni(II) by the blended resin is a spontaneous, exothermic process. The adsorption isotherm fits better to the Langmuir isotherm model and the pseudo-second-order kinetics model gives a better fit to the batch sorption kinetics. The adsorption mechanism is assumed to be ion exchange between the nickel ion and the polyamino polycarboxylic acid chelating group of the blended resin.

**Copyright © 2010 International Energy and Environment Foundation - All rights reserved.**

**Keywords:** Diethylenetriaminepentaacetic acid, Heavy metal, Kinetics equation, Polyvinylidene fluoride, Thermodynamics.

### 1. Introduction

Heavy metal contamination exists in aqueous waste effluents of many industries, such as metal plating facilities, fertilizer industry, mining operations, and tanneries. Heavy metals in the environment are not biodegradable and tend to accumulate in living organisms, causing various diseases and disorders [1]. Nickel and its compounds are ubiquitous in the environment and are, thus, found frequently in surface water. Ni<sup>2+</sup> ion is the most commonly occurring species in the environment and is toxic to living organisms. The toxicity of nickel to living organisms is essentially exerted on enzymes, because nickel, like other heavy metals, has a high affinity for ligands containing oxygen, nitrogen and sulfur donors. In China, the acceptable limit of Ni<sup>2+</sup> is 1.0 mg/L as industrial wastewater discharge [2]. Excess Ni<sup>2+</sup> may cause cancer of the lungs, nose and bone [3]. Acute nickel poisoning after ingestion may show systemic effects such as headache, dizziness, nausea and vomiting, chest pain, dry cough and extreme weakness [4].

Therefore, nickel-containing wastewater needs to be treated before discharge. Numerous processes are available for removing heavy metal ions to reduce heavy metal pollution in ecosystems, including chemical precipitation, ion exchange, carbon adsorption, coprecipitation/adsorption, and membrane filtration[5-15]. Nevertheless, many of these approaches are marginally cost effective or difficult to implement in developing countries[16-18]. Therefore, a treatment strategy is needed that is simple, robust, and that addresses local resources and constraints. One of the powerful treatment processes for the removal of metal ions from water with a low cost is adsorption. Sorption operations, including adsorption and ion exchange, are a potential alternative water and wastewater treatment technique. Conventional porous solids, such as clay, fly ash, activated carbon and silica materials, have low adsorption capacities with slow adsorption kinetics[19]. An ideal adsorbent should have accessible pore structures with uniform pore size distributions and large surface areas with physical/chemical stability and high uptake and stability[19,20]. Polyvinylidene fluoride (PVDF) has excellent mechanical and physicochemical properties with good oxidation resistance to chemical reagents, which can be used for adsorbents. However, conventional PVDF resin has no removal action on the soluble heavy metal ions. Several approaches have been developed to adhere the acrylic acid group to PVDF polymers to produce a hydrophilic surface with good ion-exchange performance[21-24]. But these techniques have drawbacks, for example, the adsorbed polymer layer is easily removed during handling and surface grafting is likely to change the polymer pore size and pore size distribution[24-27].

This study describes how the polyvinylidene fluoride blended resin (DTPA-MA/PVDF) adsorbent was prepared by anchoring the chelating agent diethylenetriaminepentaacetic acid (DTPA) to the resin via the amide covalent bond reaction between DTPA and melamine(MA), using solution blending and phase inversion techniques. The blended resin was characterized using Fourier transform infrared spectroscopy (FTIR),  $^{13}\text{C}$  nuclear magnetic resonance spectroscopy ( $^{13}\text{C}$  NMR), environmental scanning electron microscopy (ESEM) and  $\text{N}_2$  adsorption/desorption experiments. The  $\text{Ni}^{2+}$  ion sorption of the blended resin from aqueous solution was measured, along with the adsorption isotherm and the batch sorption kinetics.

## 2. Experimental

### 2.1 Materials

The PVDF powders were provided by Chen Guang Co. Ltd. (China) with a molecular weight of ca. 400000. Polyvinyl pyrrolidone (PVP) powders were supplied by the Institute of Chemical Engineering of Beijing (China). Dimethylsulfoxide (DMSO), diethylenetriaminepentaacetic acid (DTPA) and melamine(MA) were of analytical grade. All were used as received. In the current study, DTPA, MA and PVDF were used for the blended resin material. The solvent DMSO was used to prepare the blended cast solution. PVP was chosen as the pore-forming additive. A stock solution of  $\text{Ni}^{2+}$  (1000 mg/L) was prepared by dissolving appropriate amounts of  $\text{NiSO}_4 \cdot 6\text{H}_2\text{O}$  (analysis grade) in distilled water. The working solutions were prepared by diluting the stock solutions to appropriate volumes.

### 2.2 Preparation of DTPA-MA/PVDF blended resin

First, DTPA and MA powders were dissolved in DMSO solvent. The concentrations of DTPA and MA were 4.6 wt% and 4.4 wt%, respectively. The temperature of DMSO was kept at 180 °C to ensure the complete amide covalent bond reaction between DTPA and MA. The solution was cooled below 100 °C as quickly as possible when some colloidal substances were found. Then the PVDF and PVP powders were added into the aforementioned solution. The PVDF concentration was 11.5 wt%. The PVP concentration was 2.5 wt%. The solution was completely dissolved in a water bath at 70~80 °C with continuous stirring. After 3 h, the cast solution was degassed at 50~60 °C for 6 h in a water bath.

DTPA-MA/PVDF blended resin was prepared using phase inversion with distilled water as the non-solvent. The blended cast solution was dropped into distilled water from a burette to create the resin beads with diameters of 1.0~1.5 mm. After preparation, the blended resin beads were immersed in distilled water for 48 h and then the resin was soaked in 1.0 mol/L HCl solution for 24 h. Then, the beads were washed with distilled water until a neutral pH was obtained. The product was then dried at 75 °C for several hours.

### 2.3 Characterization of DTPA-MA/PVDF blended resin

After dispersion in KBr, the FTIR spectra of the pristine PVDF powder and DTPA-MA/PVDF blended resin were measured on E55+FRA106 FTIR spectrometer. Each spectrum was collected by cumulating

16 scans at a resolution of  $4\text{ cm}^{-1}$ . BRUKER AVANCE III 400 NMR spectrometry ( $^{13}\text{C}$  solid-state NMR) was used to characterize the samples of DTPA-MA/PVDF blended resin. Surface and section morphologies of the blended resin were analyzed using an ESEM (Model XL30, Philips). The  $\text{N}_2$  adsorption/desorption experiments were characterized using a Micromeritics ASAP 2010 analyzer with the pore size distributions characterized using the Barret–Joyner–Halenda (BJH) model on the desorption branch. The nickel ion sorption capacities were measured using atomic absorption spectrophotometer (AAS) for the nickel content, according to the China Standard Methods for the Examination of Water and Wastewater [28].

#### 2.4 Sorption experiments

The stock solution was diluted as required to obtain standard solutions containing 20 to 140 mg/L of  $\text{Ni}^{2+}$ . A 200 ml  $\text{Ni}^{2+}$  solution of the desired concentration, adjusted to the desired pH, was put into 250 mL reagent bottles with known amounts of the blended resin. The solution pH was adjusted using HAc-NaAc buffer solutions. All the chemicals used were of analytical reagent grade. The solutions were agitated for a predetermined period in a shaking incubator at 288K, 298K, and 308K. The sorption isotherm studies were carried out with different initial concentrations of  $\text{Ni}^{2+}$  while maintaining the adsorbent dosage at constant levels. The pH effects were measured using 100 mg/L nickel ion solutions and 0.5 g/100 mL of the blended resin. In order to correct for any adsorption of nickel on the container surface, control experiments were carried out without adsorbent. No adsorption was found to occur on the container walls. Kinetic experiments were conducted using a known weight of adsorbent with 100 mg/L  $\text{Ni}^{2+}$  at various temperatures. At various time intervals, suitable aliquots were analysed for the nickel concentration. The rate constants were calculated using a conventional rate expression. The amount of  $\text{Ni}^{2+}$  ion adsorbed by the blended resin was calculated according to equation (1)

$$q = [(C_0 - C_e)V]/W \quad (1)$$

where  $q$  is the amount of  $\text{Ni}^{2+}$  ion adsorbed onto a unit amount of the resin ( $\text{mg}\cdot\text{g}^{-1}$ ),  $C_0$  and  $C_e$  are the initial and equilibrium concentrations of  $\text{Ni}^{2+}$  ions in the aqueous phase ( $\text{mg}\cdot\text{L}^{-1}$ ),  $V$  is the volume of the aqueous phase (L) and  $W$  is the dry weight of the resin (g).

#### 2.5 Desorption experiment

The regeneration and reuse of adsorbents is an important aspect of adsorption studies. The experiments to measure the desorption efficiency were carried out with a 1.0 mol/L HCl solution. 1.0 g of the blended resin with about 11.8 mg/g nickel ions was placed into 200 mL of HCl solution with agitation. The desorption was quantified by measuring the nickel ion concentrations in the solution for various times up to equilibrium. The desorption efficiency was expressed as equation (2)

$$\text{DE} = (q_1/q_0) \times 100\% \quad (2)$$

where  $q_1$  is the desorbed amount of  $\text{Ni}^{2+}$  ion from the resin ( $\text{mg}\cdot\text{g}^{-1}$ ) and  $q_0$  is the adsorbed amount of  $\text{Ni}^{2+}$  ion on the resin at equilibrium ( $\text{mg}\cdot\text{g}^{-1}$ ). To examine the reusability of the blended resin, the adsorption-desorption process was repeated for four cycles with the adsorption performance analyzed in each cycle. The adsorption was conducted with 1.0 g of resin in 200 mL of 100 mg/L initial nickel ion concentration at pH 6.6. During the adsorption and desorption processes, the solution temperature was kept as 298 K.

### 3 Results and discussion

#### 3.1 Characterization of DTPA-MA/PVDF blended resin

##### 3.1.1 FTIR analysis of DTPA-MA/PVDF blended resin

In order to investigate the complex formation in the DTPA-MA/PVDF blended resin, FTIR studies have been carried out. FTIR spectra of the pristine PVDF resin and DTPA-MA/PVDF resin are shown in Figure 1. The absorption peaks appearing at  $3025$ ,  $471$  and  $1200\text{cm}^{-1}$  are assigned to PVDF C-F stretching, wagging, and bending vibration modes, respectively[29], which are found to be weak in the DTPA-MA/PVDF resin. The peak at  $1552\text{ cm}^{-1}$  can be assigned to N-H bend of bridging secondary amine of the blended resin, and the peak at  $1493\text{ cm}^{-1}$  can be attributed to the methylene C-H bend of the blended resin[30]. The  $-\text{OH}$  bending vibration of  $-\text{COOH}$  group of DTPA appears at  $1340\text{cm}^{-1}$ . The

reported absorption peak at  $1636\text{ cm}^{-1}$  is assigned to C=O mode of amide group[30], which is shifted to  $1670\text{ cm}^{-1}$  in the blended resin. The FTIR spectra clearly demonstrate that the polyamino polycarboxylic acid functional group has been blended to PVDF resin successfully.

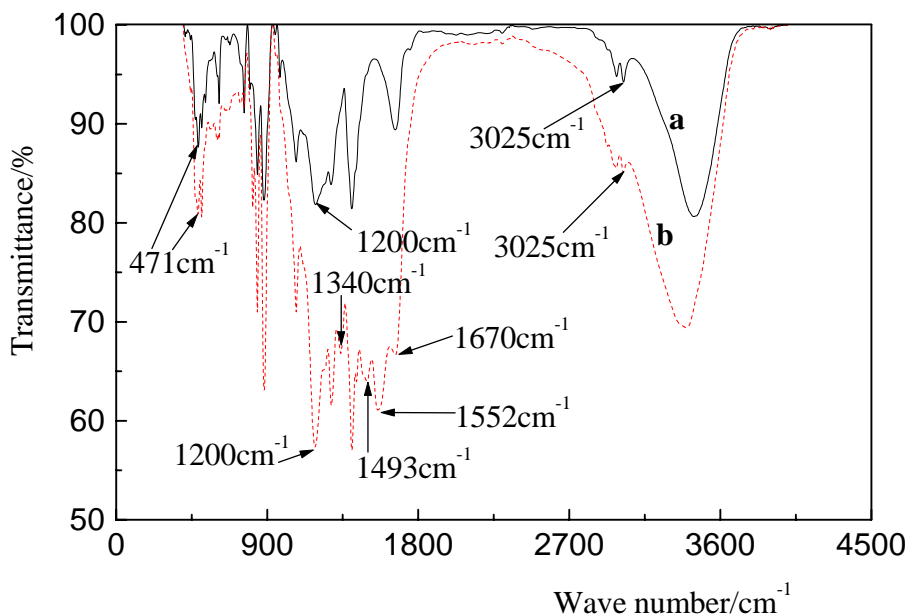


Figure 1. FTIR spectra of the resins: (a) pristine PVDF, (b) DTPA-MA/PVDF

### 3.1.2 $^{13}\text{C}$ solid-state NMR analysis of DTPA-MA/PVDF blended resin

$^{13}\text{C}$  solid-state NMR spectra of PVDF and DTPA-MA/PVDF resins are shown in Figure 2. The signals at 20.1 ppm and 33.1 ppm can be assigned to adamantane which is used as the internal standard. The signals which appears at 44.6 ppm and 121.8 ppm for PVDF can be assigned to  $-\text{CH}_2-$  and  $-\text{CF}_2-$  groups[30], respectively. By a comparison of curve a with b in Figure 2, it can be seen there are three new signals at 56.0 ppm, 158.7 ppm and 168.5 ppm in DTPA-MA/PVDF resin. The signal which appears at 56.0 ppm is assigned to  $-\text{CH}_2\text{N}-$  group of DTPA and the signal at 158.7 ppm can be assigned to the three carbons in the triazine ring of MA. A high frequency signal appears at 168.5 ppm for the blended resin, and strongly relates to carbonyl carbon of amide and/or carboxylic groups[31]. The polyamino polycarboxylic acid chelating group has been blended to PVDF resin, and it can be inferred that DTPA-MA/PVDF resin should possess a considerable adsorption capacity of  $\text{Ni}^{2+}$  ion.

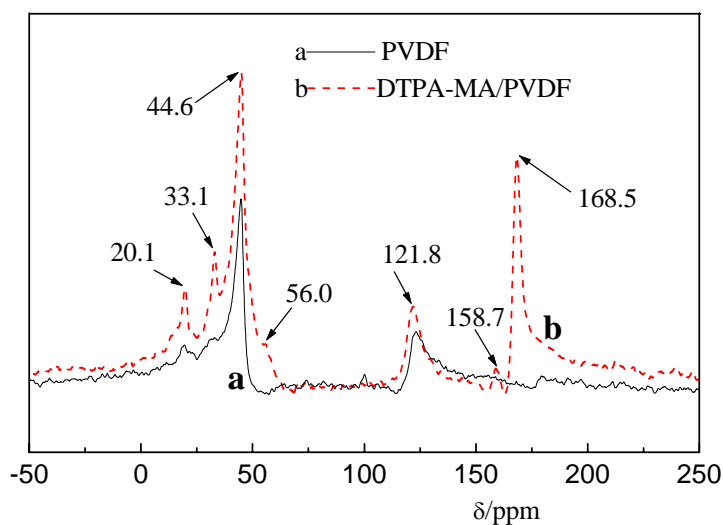
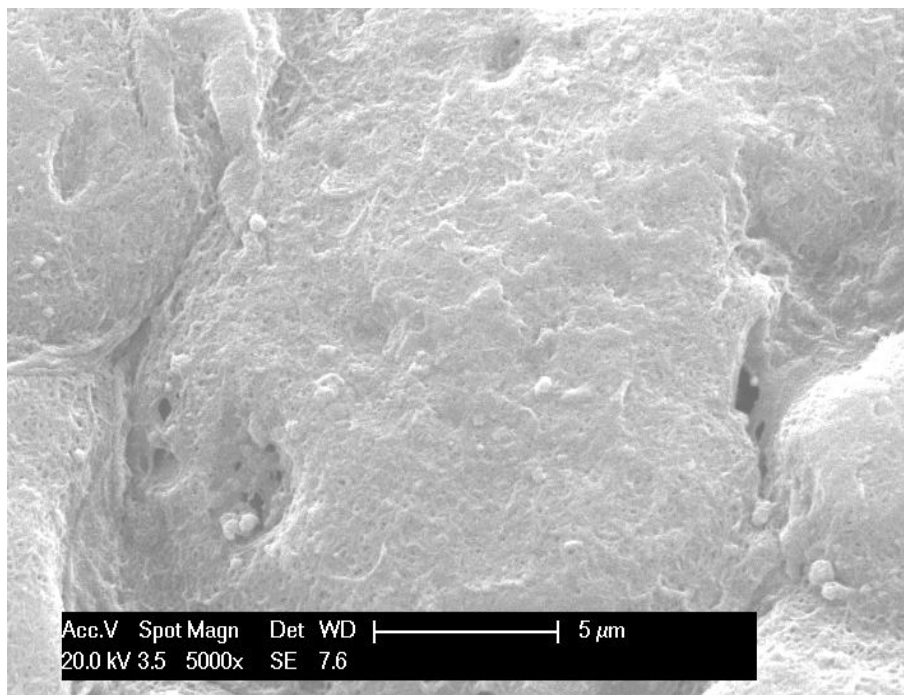


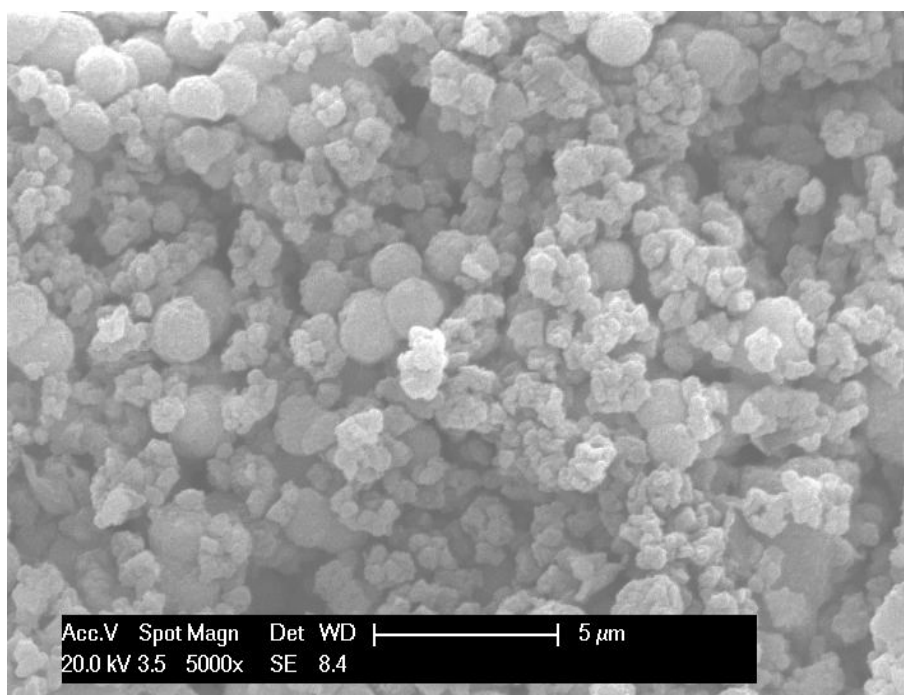
Figure 2.  $^{13}\text{C}$  NMR of the resins: (a) pristine PVDF, (b) DTPA-MA/PVDF

### 3.1.3 Surface and section morphologies of DTPA-MA/PVDF blended resin

The surface and section morphologies of DTPA-MA/PVDF blended resin were measured using ESEM. SEM micrographs of the resin are shown in Figure 3. The micrograph in Figure 3a shows that pores are distributed on the exterior surface of the blended resin with larger pores on the polymer surface and many smaller pores in the interior. The micrograph in Figure 3b further shows that many pores are distributed in the interior of the blended resin. When the blended resin is immersed into the  $\text{Ni}^{2+}$  solution, the  $\text{Ni}^{2+}$  ion will diffuse into the resin through the pores in the exterior and interior surfaces of the blended resin. Thus, the blended resin has a high  $\text{Ni}^{2+}$  ion adsorption capacity.



(a) Surface photograph

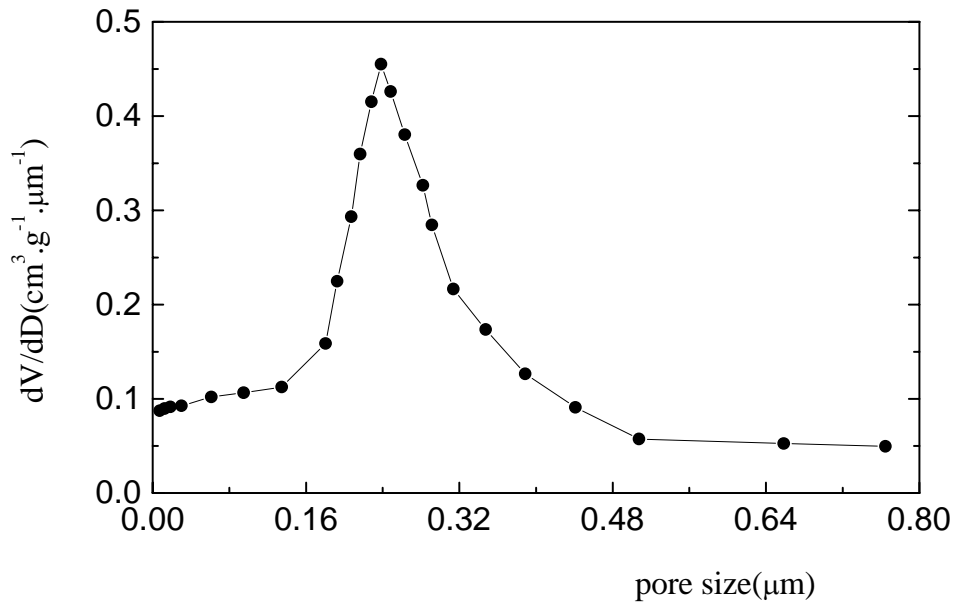


(b) Section photograph

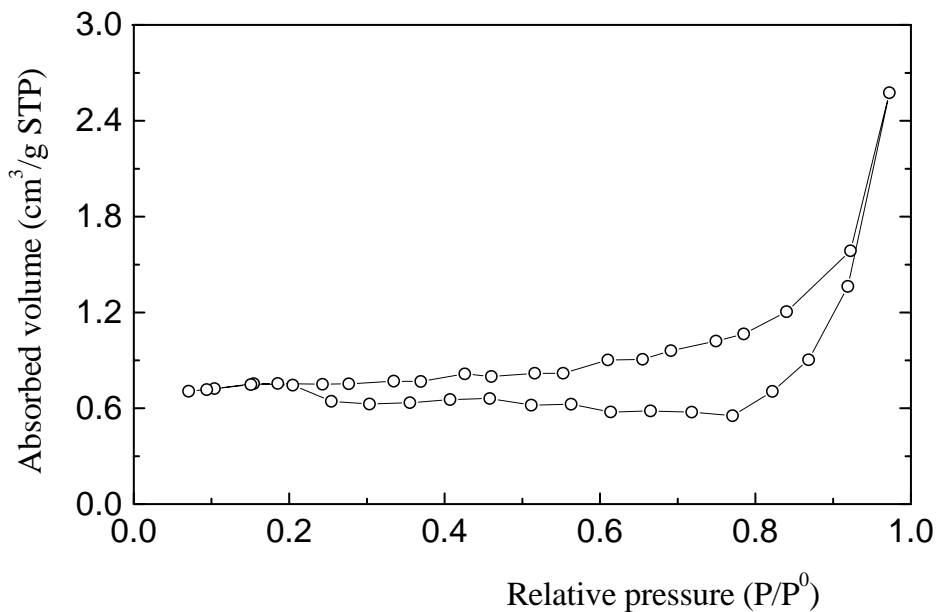
Figure 3. SEM of the DTPA-MA/PVDF blended resin

### 3.1.4 Specific surface area and pore size distribution in DTPA-MA/PVDF blended resin

The specific surface area and the pore size distribution of DTPA-MA/PVDF blended resin were characterized by  $N_2$  adsorption/desorption tests. As shown in Figure 4a, the resin bead had a narrow pore size distribution with a mean pore diameter of  $0.24 \mu\text{m}$  and a specific surface area of  $2.43 \text{ m}^2/\text{g}$ . The location of the hysteresis loop in the  $N_2$  isotherm shown in Figure 4b can be used to determine whether the blended resin possesses a regular framework of pores or interparticle voids, such as textural pores. The framework porosity at  $0.2\text{-}0.9 P/P^0$  ( $P/P^0$  denoted as the relative pressure) on the  $N_2$  isotherm indicates the porosity is contained in relatively uniform channels of the templated framework, while the textural porosity at  $0.9\text{-}1.0 P/P^0$  shows the porosity arising from the noncrystalline intra-aggregate voids and spaces formed by interparticle contact [18]. Thus, the blended resin shows the presence of both framework porosity and textural porosity. This suggests that the blended resin has a regular pore size distribution.



(a) Pore size distribution



(b) Isotherm

Figure 4.  $N_2$  adsorption/desorption curve for the blended resin

### 3.2 Effects of pH and initial $Ni^{2+}$ concentration on the $Ni^{2+}$ adsorption

The pH of a solution is an important parameter affecting adsorption processes because of the pH dependency of complexation reactions and electrostatic interactions at the adsorption surface[32]. Since the structure of the blended resin has the polyamino polycarboxylic acid chelating group, the pH dependencies of the  $Ni^{2+}$  ion have to be determined. The effect of pH on the adsorption capacities of  $Ni^{2+}$  were examined by varying the initial pH of the solutions. The solution temperature was set to 298 K for all the tests measuring and the variation of the metal uptake with pH is shown in Figure 5. The adsorption capacities are found to be low at lower pH and to increase with increasing pH due to competitive adsorption between the  $H^+$  ion and the  $Ni^{2+}$  ion for the same active adsorption site. As the pH increases, the adsorption surface becomes less positive, so the electrostatic attraction between the  $Ni^{2+}$  ion and resin surface increases. The increased adsorption with pH may be further explained in terms of the polyamino polycarboxylic acid chelating group on the resin. The functional group probably takes part in the  $Ni^{2+}$  uptake process by a chelating complexation reaction which is pH-dependent, and the nature of the active sites and  $Ni^{2+}$  ion may change with pH[33]. The optimum pH which gives the maximum  $Ni^{2+}$  uptake is 6.0~7.0.

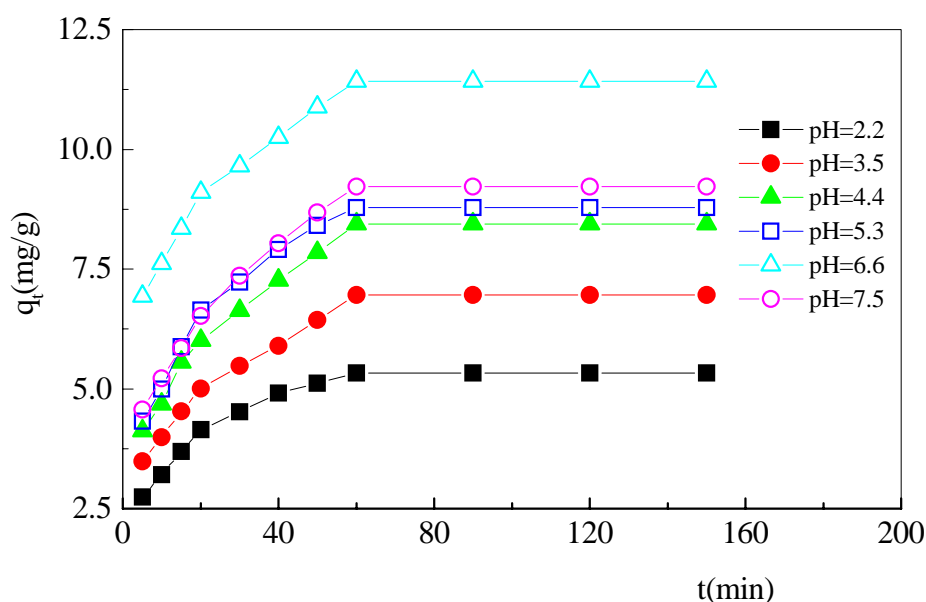


Figure 5. Effect of pH on the adsorption of  $Ni^{2+}$  ions

The effect of the initial  $Ni^{2+}$  concentration on the  $Ni^{2+}$  adsorption capacity of the blended resin at 298 K and pH 6.6 was studied with 7 g/L of blended resin and a contact time of 2 h. The results in Table 1 show that with increasing initial  $Ni^{2+}$  concentration, the equilibrium adsorption capacity ( $q_e$ ) of the resin increases, but the residual  $Ni^{2+}$  concentration is higher and the  $Ni^{2+}$  removal rate decreases.

Table 1. Effect of initial  $Ni^{2+}$  concentration on the resin's adsorption capacity

Initial $Ni^{2+}$ / ( $mg \cdot L^{-1}$ )	Residual $Ni^{2+}$ / ( $mg \cdot L^{-1}$ )	$q_e$ / ( $mg \cdot g^{-1}$ )	$Ni^{2+}$ removal / (%)
19.25	2.18	2.56	88.68
39.28	5.68	5.04	85.54
59.74	10.47	7.39	82.47
79.37	16.23	9.47	79.55
103.39	24.32	11.86	76.48
119.65	31.52	13.22	73.66
139.42	42.02	14.61	69.86

### 3.3 Effect of contact time and sorption kinetics

The  $Ni^{2+}$  ion uptake capacities were measured as a function of time to determine the optimum contact time for the adsorption of  $Ni^{2+}$  ion on the blended resin. Figure 6 shows the time course of the adsorption

equilibrium of  $\text{Ni}^{2+}$  ions onto the blended resin. There is rapid uptake for the first 60 min with adsorption equilibrium attained within 120 min. Actually, the adsorption is very close to equilibrium within the first 90 min. Therefore, 2 h of contact time was chosen as the optimum equilibration time for the experimental studies, unless otherwise stated, to ensure that equilibrium was achieved.

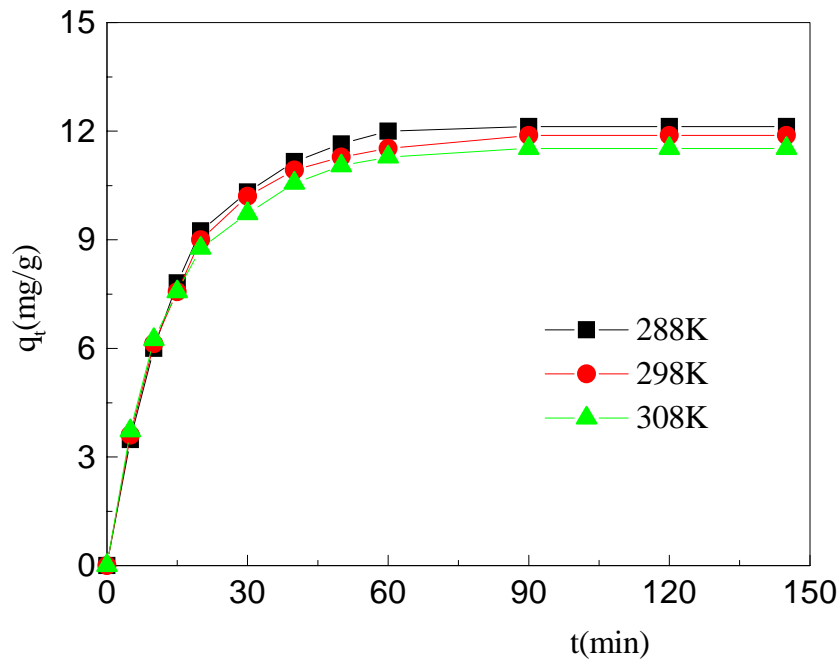


Figure 6. Effects of contact time and temperature on the adsorption of  $\text{Ni}^{2+}$  ions

Adsorption processes are controlled by various mechanisms, such as mass transfer, mass diffusion, chemical reactions and particle diffusion. To clarify the mechanisms controlling the adsorption, several adsorption models were used to evaluate the experimental data. The kinetics were compared to a pseudo-first-order kinetic model, a pseudo-second-order kinetic model and an intraparticle diffusion model. The calculated  $q_e$  and correlation coefficients ( $R^2$ ) for various temperatures are summarized in Table 2, where  $k_{p1}$ ,  $k_{p2}$  and  $k_{id}$  is the rate constant of pseudo-first-order kinetic model ( $\text{min}^{-1}$ ), pseudo-second-order kinetic model ( $\text{g} \cdot (\text{mg} \cdot \text{min})^{-1}$ ) and intraparticle diffusion model ( $\text{mg} \cdot (\text{g} \cdot \text{min}^{1/2})^{-1}$ ), respectively, and  $T$  is the temperature. The data indicates that the kinetics of the pseudo-second-order kinetics model better represents the experimental data than the pseudo-first-order rate model or the intraparticle diffusion model.

Table 2. First-order, second-order and intraparticle diffusion rate constants

T/K	Pseudo-first-order kinetic model			Pseudo-second-order kinetic model			Intraparticle diffusion model	
	$k_{p1}$ ( $\text{min}^{-1}$ )	$q_e$ ( $\text{mg} \cdot \text{g}^{-1}$ )	$R^2$	$k_{p2}$ [ $\text{g} \cdot (\text{mg} \cdot \text{min})^{-1}$ ]	$q_e$ ( $\text{mg} \cdot \text{g}^{-1}$ )	$R^2$	$k_{id}$ [ $\text{mg} \cdot (\text{g} \cdot \text{min}^{1/2})^{-1}$ ]	$R^2$
288	0.0566	16.2836	0.9983	0.0061	14.8038	0.9984	1.3883	0.9530
298	0.0613	10.9206	0.9765	0.0055	14.1743	0.9989	1.3108	0.9532
308	0.0717	10.2125	0.9889	0.0045	13.5906	0.9996	1.2283	0.9581

### 3.4 Effect of temperature and sorption isotherms

The effect of temperature on the  $\text{Ni}^{2+}$  ion uptake was investigated by varying the temperature of the solution with pH as 6.6. The data in Figure 6 shows that the adsorption capacity increases with increasing temperature to a plateau which represents the maximum adsorption capacity of the blended resin. This increase in loading capacity of the resin with temperature represents an exothermic process. The equilibrium adsorption capacity of  $\text{Ni}^{2+}$  on the blended resin at 288 K is 12.12 mg/g, at 298 K is 11.88 mg/g, and at 308K is 11.52 mg/g.

The isotherm data can be used to develop an equation for design purposes. The experimental data for the effect of temperature on the adsorption capacity was evaluated relative to the three popular adsorption models, the Langmuir, Freundlich and D-R models. In Table 3,  $q_m$  is the maximum sorption capacity ( $\text{mg}\cdot\text{g}^{-1}$ ),  $K_a$  is the Langmuir constant ( $\text{L}\cdot\text{g}^{-1}$ ), and  $E$  is the mean free energy of adsorption ( $\text{kJ}\cdot\text{mol}^{-1}$ ). The results listed in Table 3 show that the  $\text{Ni}^{2+}$  ion sorption isotherms can be explained by all three models but that the Langmuir equation gives the best fit. This result also predicts the mono-molecular layer of the adsorption sites on the blended resin. The Freundlich constant,  $K_F$ , indicates the sorption capacity of the resin. As can be seen from Table 3,  $K_F$  was 7.45 at 288 K, 7.21 at 298 K and 6.75 at 308 K for the  $\text{Ni}^{2+}$  adsorption. The heterogeneity factor  $n$  were all found to be greater than 1. This result is very common and may be due to the distribution of surface sites or other factors that reduce the adsorbent–adsorbate interaction with increasing surface density [34]. The D-R isotherm model results show that the mean free energy of adsorption ( $E$ ) is between 8 and 16 kJ/mol, so it is possible that the adsorption  $\text{Ni}^{2+}$  ions on the blended resin can be explained as an ion-exchange process[35].

Table 3. Langmuir, Freundlich and D-R isotherm constants

T/K	Langmuir isotherm			Freundlich isotherm			D-R isotherm		
	$q_m/(\text{mg}\cdot\text{g}^{-1})$	$K_a/(\text{L}\cdot\text{g}^{-1})$	$R^2$	$K_F$	$n$	$R^2$	$q_m/(\text{mg}\cdot\text{g}^{-1})$	$E/(\text{kJ}\cdot\text{mol}^{-1})$	$R^2$
288	15.7903	0.1325	0.9974	7.4526	6.7431	0.9867	24.9115	15.08	0.9924
298	15.3917	0.1313	0.9975	7.2124	6.6489	0.9929	23.6979	15.93	0.9929
308	14.8610	0.1312	0.9983	6.7473	6.3012	0.9951	23.5064	15.93	0.9993

The thermodynamic parameters such as the standard free energy change ( $\Delta G^\circ$ ), standard enthalpy change ( $\Delta H^\circ$ ), and standard entropy change ( $\Delta S^\circ$ ) were estimated[35,36].

$$\log K_D = -\frac{\Delta H^\circ}{2.303RT} + \frac{\Delta S^\circ}{R} \quad (3)$$

$$\Delta G^\circ = \Delta H^\circ - T\Delta S^\circ \quad (4)$$

where  $K_D$  is the distribution coefficient ( $\text{mL}\cdot\text{g}^{-1}$ ), and  $R$  is the gas constant ( $\text{kJ}\cdot\text{mol}^{-1}\cdot\text{K}^{-1}$ ). The calculated thermodynamic parameters are listed in Table 4.  $\Delta H^\circ$  is negative for all cases due to the exothermic nature of the adsorption. The negative  $\Delta G^\circ$  indicates the spontaneous nature of the reaction and the decreasingly negative  $\Delta G^\circ$  with temperature indicates that the reaction is more favored at lower temperatures. The values of  $\Delta S^\circ$  are positive due to the exchange of  $\text{Ni}^{2+}$  ions with more mobile ions on the resin, which increases the entropy during the adsorption process[37]. The values in Table 4 show that the adsorption of  $\text{Ni}^{2+}$  by the blended resin is a spontaneous, exothermic process.

Table 4. Thermodynamic parameters for the adsorption of  $\text{Ni}^{2+}$  on the blended resin

T/K	$\Delta G^\circ/(\text{kJ}\cdot\text{mol}^{-1})$	$\Delta H^\circ/(\text{kJ}\cdot\text{mol}^{-1})$	$\Delta S^\circ/(\text{J}\cdot\text{mol}^{-1}\cdot\text{K}^{-1})$
288	-7.71	—	—
298	-7.88	-2.69	17.40
308	-8.05	—	—

### 3.5 Desorption of the blended resin

Good desorption of an adsorbent is important for potential practical applications. Figure 7 shows the amount of nickel ions adsorbed on DTPA-MA/PVDF blend resin in four adsorption/desorption cycles. The results show that the blended resin still has good adsorption/desorption capability. After four cycles, the adsorption capacity of the blended resin is greater than 11 mg/g and its desorption efficiency is above 90%. Therefore, the blended resin can be reused without any significant loss in the adsorption performance. Therefore, for the further research on the blended resin should be done, such as the treatment of the nickel plating spent solutions.

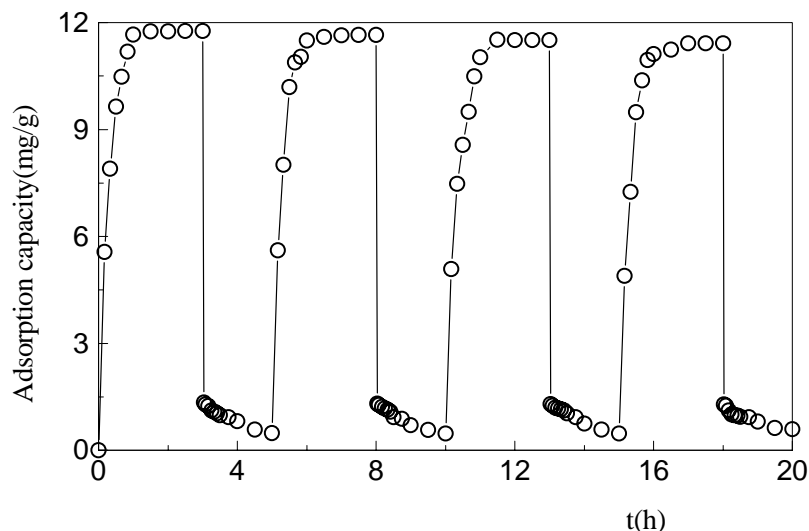


Figure 7. Repeated adsorption /desorption curves for DTPA-MA/PVDF blended resin

#### 4. Conclusions

A blended resin containing the polyamino polycarboxylic acid chelating group was synthesized for the adsorption of  $\text{Ni}^{2+}$  ions. Experimental results show that the resin effectively removes nickel ions in synthetic solutions for pH from 2 to 7. Adsorption on the blended resin is best modeled by the Langmuir adsorption isotherms model, which shows the mono-molecular layer characteristics of the adsorption sites on the resin. The adsorption of  $\text{Ni}^{2+}$  ions onto the blended resin was found to be an ion-exchange process. The adsorption process was found to be an exothermic, spontaneous, and pseudo-second-order kinetic process. This blended resin can be used to treat waste to reduce environmental pollution and deserves further extensive study.

#### References

- [1] Aaseth J., Norseth T. Handbook on the Toxicity of Metals. Elsevier, Netherlands, 1986.
- [2] Chinese wastewater emission Standard, GB 8978-1996.
- [3] Parker S.P. Encyclopedia of Environmental Science, second ed., McGraw-Hill, New York, 1980.
- [4] Beliles R.P. The lesser metals, in: F.W. Oehme (Ed.), Toxicity of Heavy Metals in the Environment. Part 2, Marcel Dekker, New York, 1979, pp. 547-616.
- [5] Xu D., Zhou X., Wang X.K. Adsorption and desorption of  $\text{Ni}^{2+}$  on Na-montmorillonite: Effect of pH, ionic strength, fulvic acid, humic acid and addition sequences. J. Applied Clay Science. 2008, 39(3-4), 133-141.
- [6] Su H.J., Chen S., Tan T.W. Surface active site model for  $\text{Ni}^{2+}$  adsorption of the surface imprinted adsorbent. J. Process Biochemistry. 2007, 42(4), 612-619.
- [7] Li Q., Su H.J., Li J., Tan T.W. Application of surface molecular imprinting adsorbent in expanded bed for the adsorption of  $\text{Ni}^{2+}$  and adsorption model. J. Env. Manag.. 2007, 85(4), 900-907.
- [8] Donat R., Akdogan A., Erdem E., Cetisli H. Thermodynamics of  $\text{Pb}^{2+}$  and  $\text{Ni}^{2+}$  adsorption onto natural bentonite from aqueous solutions. J. Colloid and Interface Science, 2005, 286(1), 43-52.
- [9] Hsu T.C. Experimental assessment of adsorption of  $\text{Cu}^{2+}$  and  $\text{Ni}^{2+}$  from aqueous solution by oyster shell powder. J. Hazardous Materials. 2009, 171(1-3), 995-1000.
- [10] Kang S.Y., Lee J.U., Moon S.H., Kim K.W. Competitive adsorption characteristics of  $\text{Co}^{2+}$ ,  $\text{Ni}^{2+}$ , and  $\text{Cr}^{3+}$  by IRN-77 cation exchange resin in synthesized wastewater. J. Chemosphere. 2004, 56(2), 141-147.
- [11] Rengaraj S., Yeon K.H., Kang S.Y., Lee J.U., Kim K.W., Moon S.H. Studies on adsorptive removal of Co(II), Cr(III) and Ni(II) by IRN77 cation-exchange resin. J. Hazardous Materials. 2002, 92(2), 185-198.
- [12] Vieira M., Tavares C.R., Bergamasco R., Petrus J.C.C. Application of ultrafiltration-complexation process for metal removal from pulp and paper industry wastewater. J. Membrane Sc. 2001, 194(2), 273-276.
- [13] Marty J., Persin M., Sarrazin J. Dialysis of Ni(II) an ultra-filtration enhanced by polymer complexation. J. Membrane Science. 2000, 167(2), 291-297.

- [14] Durham B., Bourbigot M., Pankratz T. Membranes as pretreatment to desalination in wastewater reuse: operating experience in the municipal and industrial sectors. *J. Desalination*. 2001, 138(1-3), 83-90.
- [15] Durham B., Bourbigot M.M., Pankratz T. Membranes as pretreatment to desalination in wastewater reuse. *J. Membrane Technology*. 2002, 143(5), 8-12.
- [16] Pehlivan E., Altun T. The study of various parameters affecting the ion exchange of  $\text{Cu}^{2+}$ ,  $\text{Zn}^{2+}$ ,  $\text{Ni}^{2+}$ ,  $\text{Cd}^{2+}$ , and  $\text{Pb}^{2+}$  from aqueous solution on Dowex50W synthetic resin. *J. Journal of Hazardous Materials*. 2006, 134(1-3), 149-156.
- [17] Kadirvelu K., Namasivayam C. Activated carbon from coconut coirpith as metal adsorbent: adsorption of Cd(II) from aqueous solution. *J. Advances in Environmental Research*. 2003, 7(2), 471-478.
- [18] Chan W.C., Fu T.P. Adsorption/ion-exchange behaviour between a water-insoluble cationic starch and 2-chlorophenol in aqueous solutions. *J. Applied Polymer Science*. 1998, 67(6), 1085-1092.
- [19] Rengaraj S., Kim Y., Joo C.K., Yi J. Removal of copper from aqueous solution by aminated and protonated mesoporous aluminas: kinetics and equilibrium. *J. Journal of Colloid and Interface Science*. 2004, 273(1), 14-21.
- [20] Lee B., Kim Y., Lee H., Yi J. Synthesis of functionalized porous silicas via templating method as heavy metal ion adsorbents: the introduction of surface hydrophilicity onto the surface of adsorbents. *J. Microporous and Mesoporous Materials*. 2001, 50(1), 77-90.
- [21] Jorngong S.K., Phunchareon P. Influence of reaction parameters on water absorption of neutralized poly(acrylic-co-acrylamide) synthesized by inverse suspension polymerization. *J. Journal of Applied polymer Science*. 1999, 72(10), 1349-1366.
- [22] Chen J.W., Zhao Y.M. Relation between water absorbency and reaction conditions in aqueous solution polymerization of polyacrylate super absorbents. *J. Journal of Applied polymer Science*. 2000, 75(6), 808-814.
- [23] Mazzei R.O., Bermúdez G.G., Tadey D., Rocco C. Grafting of poly(vinylidene fluoride) foils induced by swift heavy ions. *J. Nuclear Instruments and Methods in Physics Research Section B: Beam Interactions with Materials and Atoms*. 2004, 218, 313-317.
- [24] Betz N., Begue J., Goncalves M., Gionnet K., Déléris, Moël A.L. Functionalisation of PAA radiation grafted PVDF. *J. Nuclear Instruments and Methods in Physics Research Section B: Beam Interactions with Materials and Atoms*, 2003, 208, 434-441.
- [25] Gancarz I., Pozniak G., Bryjak M., Frankiewicz A. Modification of polysulfone membranes. 2. Plasma grafting and plasma polymerization of acrylic acid. *J. Acta Polymerica*. 1999, 50(9), 317-326.
- [26] Ying L., Kang E.T., Neoh K.G. Characterization of membranes prepared from blends of poly(acrylic acid)-graft-poly(vinylidene fluoride) with poly(N-isopropylacrylamide) and their temperature and pH-sensitive microfiltration. *J. Membrane Science*. 2003, 224(1-2), 93-106.
- [27] Clochard M.C., Bègue J., Lafon A., Caldemaison D., Bittencourt C., Pireaux J.J., Betz N. Tailoring bulk and surface grafting of poly(acrylic acid) in electron-irradiated PVDF. *J. Polymer*. 2004, 45(26), 8683-8694.
- [28] Chinese Environmental Protection Standard Edition: Water Quality Monitoring Standard, Chinese Standard Press, Beijing, China, 2001.
- [29] Song L.Z., Dong C.Y., Li J. Application of the PAA-PVDF microfiltration composite membrane for municipal wastewater advanced treatment. *J. Toxicological Env. Chem*. 2007, 89(2), 223-232.
- [30] Qiu G.M., Zhu L.P., Zhu B.K., Xu Y.Y., Qiu G.L. Grafting of styrene/maleic anhydride copolymer onto PVDF membrane by supercritical carbon dioxide: Preparation, characterization and biocompatibility. *J. The Journal of Supercritical Fluids*. 2008, 45(3), 374-383.
- [31] Baraka A., Hall P. J., Heslop M. J. Preparation and characterization of melamine-formaldehyde-DTPA chelating resin and its use as an adsorbent for heavy metals removal from wastewater. *J. Reactive and Functional Polymers*. 2007, 67(7), 585-600.
- [32] Taty-Costodes V.C., Fauduet H., Porte C., Delacroix A. Removal of Cd(II) and Pb(II) ions from aqueous solutions by adsorption onto sawdust of *Pinus sylvestris*. *J. Hazardous Materials*. 2003, 105(1), 121-142.
- [33] Kantipuly C., Katragadda S., Chow A., Gesser H.D. Chelating polymers and related supports for separation and preconcentration of trace metals. *J. Talanta*. 1990, 37(5), 491-517.

- [34] Ünlü N., Ersoz M. Adsorption characteristics of heavy metal ions onto a low cost biopolymeric sorbent from aqueous solutions. *J. Hazardous Materials*. 2006, 136(2), 272-280.
- [35] Bering B.P., Dubinin M.M, Serpinsky V.V. On thermodynamics of adsorption in micropores. *J. Colloid and Interface Science*. 1972, 38(1), 185-194.
- [36] Mohan D., Singh K.P. Single- and multi-component adsorption of cadmium and zinc using activated carbon derived from bagasse-an agricultural waste. *J. Water Research*. 2002, 36(9), 2304-2318.
- [37] Kilislioglu A., Bilgin B. Thermodynamic and kinetic investigations of uranium adsorption on amberlite IR-118H resin. *J. Applied Radiation and Isotopes*. 2003, 58(2), 155-160.



**Xiaodan Zhao:** a post graduate majoring in environmental engineering in Yanshan University situated in Qinhuangdao, China. Wastewater treatment is her current study field.  
E-mail address: zhaoxd\_1987@163.com



**Laizhou Song:** a professor in Yanshan University with a Ph.D in applied chemistry. He is engaged in the wastewater treatment and new energy application, and has published some related articles and patents in this field.  
E-mail address: songlz@ysu.edu.cn; Tel: 86-335-8061569.



**Jun He:** an instructor in Yanshan University with a master degree in environmental science. Wastewater treatment is his current study field.  
E-mail address: hejun@ysu.edu.cn



**Tingying Wu:** a post graduate majoring in environmental engineering in Yanshan University. Wastewater treatment is her current study interest.  
E-mail address: wutingying\_1983@sina.com



**Ying Qin:** an undergraduate majoring in environmental engineering in Yanshan University.  
E-mail address: qinying\_2007@yahoo.cn